Article

Half dome-shaped carbon nitride nanostructures

Alessandro La Torre *

Posted Date: 25 September 2023

doi: 10.20944/preprints202309.1317.v2

Keywords: Ostwald, chains, cyanopolyynes, carbon nitride, half dome

Article

Half Dome Carbon Nitride Nanostructures

A. La Torre [1,2,3]

[1] ALT Carbotecnologia srls and Carbastrial limited, Via Del Nuovo Tiro a Segno 15/1 Pescara, 65128, Italy, virtual office at 16 Bridge Street Kington Herefordshire HR5 3DJ, UK; alessandro-latorre@hotmail.it
[2] Institut de Physique et Chimie des Matériaux de Strasbourg, UMR 7504 CNRS, Université de Strasbourg, 23 rue du Loess, 67034 Strasbourg, France.
[3] University of Nottingham, School of Chemistry, University Park, Nottingham, NG72RD, UK.

Abstract: We report on a new form of nanoscale carbon nitride in the shape of single layer half dome structures grown on the step edges of boron nitride sheets. The half dome structures are formed spontaneously at high temperature using Fe_2O_3 capped with $N(CH_3)_4OH$ supported on BN sheets. During the combustion process the support, firstly, acted as a reducing agent for the transformation of the iron oxide in metallic iron, secondly, as a source of nitrogen that permitted the transformation of the organic capping agent in sp^1 CN chains linked with sp^2 CN domains. During the Ostwald ripening processes smaller nanoparticles migrates towards bigger nanoparticle, when the nanoparticles come across the step edges of few layer boron nitrides sheets the half dome structure is formed. This new method of synthesis has demonstrated for the first time the formation of half dome structures containing cyanopolyynes sp^1 CN chains which link with CN sp^2 domains.

Keywords: Ostwald; chains; cyanopolyynes; carbon nitride; half dome

Introduction

Carbon is able to form a wide variety of stable structures including diamond, graphite, fullerenes, nanotubes, onions, amorphous materials, ribbons, carbon chains, carbon flowers, nano sponges all of which consist of a network of carbon atoms in different hybridisation states, sp^3, sp^2 or sp^1, intermixed in different proportions.[1-7] For instance, carbon nanotubes and graphene consist of primarily sp^2-hybridised carbon, with a small proportion of sp^3- or sp^1-hybridised carbon atoms at sites of defects or along the edges,[8-11] where as nanodiamonds that primarily comprise sp^3-hybridised carbon often contain some sp^2-hybridised carbon atoms on the surface.[12] Furthermore, due to a sharp nanoscale curvature of some carbon materials, the atoms may exist in intermediate hybridisation states, such as the case of C_{60} fullerene where carbon is neither sp^2 nor sp^3-hybridised.[13]

In recent years, atomic carbon chains have acquired much attention as they are considered to be the ultimate nanowire, *i.e.* mechanically robust,[14] highly conducting[15-17] and with tuneable electronic properties.[15-17] Isolated carbon and boron nitride chains have been shown to be stable in vacuum inside the column of a transmission electron microscope (TEM) or encapsulated within carbon nanotubes.[18-21] However, in bulk, the atomic chains are expected to be highly unstable and undergo cross-linking[22] with methodologies for the controlled fabrication and stabilisation of pure carbyne remaining inaccessible.

In this study, we have demonstrated a new form of nanoscale species in the shape of half dome structures (CN@HDS) with the bonding characteristics of either sp^1 or sp^2 carbon nitride. The CN@HDS are formed spontaneously at high temperature in a dedicated heating stage in a transmission electron microscope from $N(CH_3)_4OH$ adsorbed on the surface of colloidal Fe_2O_3 nanoparticles during the combustion Fe_2O_3 is reduced to Fe. The capping agent (surfactant) was still strongly bonded to the surfaces of the nanoparticles while it was reacting with few layer boron nitride sheets to form the CN@HDS. This new method of synthesis has demonstrated unprecedented levels of control over the CN@HDS formation, as thermally driven Ostwald ripening and particles migration of the metal particle provides for precise control of the CN@HDS, whilst the propensity of FeNPs to catalyse the formation of CN@HDS containing cynapolyynes species has been shown for

Preprints (www.preprints.org) | NOT PEER-REVIEWED | Posted: 25 September 2023 doi:10.20944/preprints202309.1317.v2

the first time. The coexistence of carbon nitride atoms in two well-defined hybridisation states within the CN@HDS may offer functional features characteristic of carbyne (tuneable electronic band gap) and graphene (high mobility of charge carriers) as they can also be grown on graphene, thus opening a wealth of opportunities for practical applications as miniaturized opto-electronic, computing devices, and gas storage devices.[23-31]

Results

Hexagonal boron nitride sheets (of lateral size 50-200 nm and thickness 1-10 layers) (FLBN) deposited on a gold mesh finder grid of a TEM were heated in air at 500 °C to remove adventitious carbon. Iron oxide nanoparticles Fe_2O_3 (average size of 11.2 ± 0.5 nm) capped with tetra methyl ammonium hydroxide $N(CH_3)_4OH$ were deposited from solution onto freshly FLBN sheets on a TEM grid (Figure 1 and S2a). Raman spectroscopy carried out on freshly FLBN showed (Figure S1) a single sharp band at 1363 cm^{-1} characteristic of an h-BN phase and the EELS analysis confirmed the absence of advantageous carbon (Figure S2).[32]

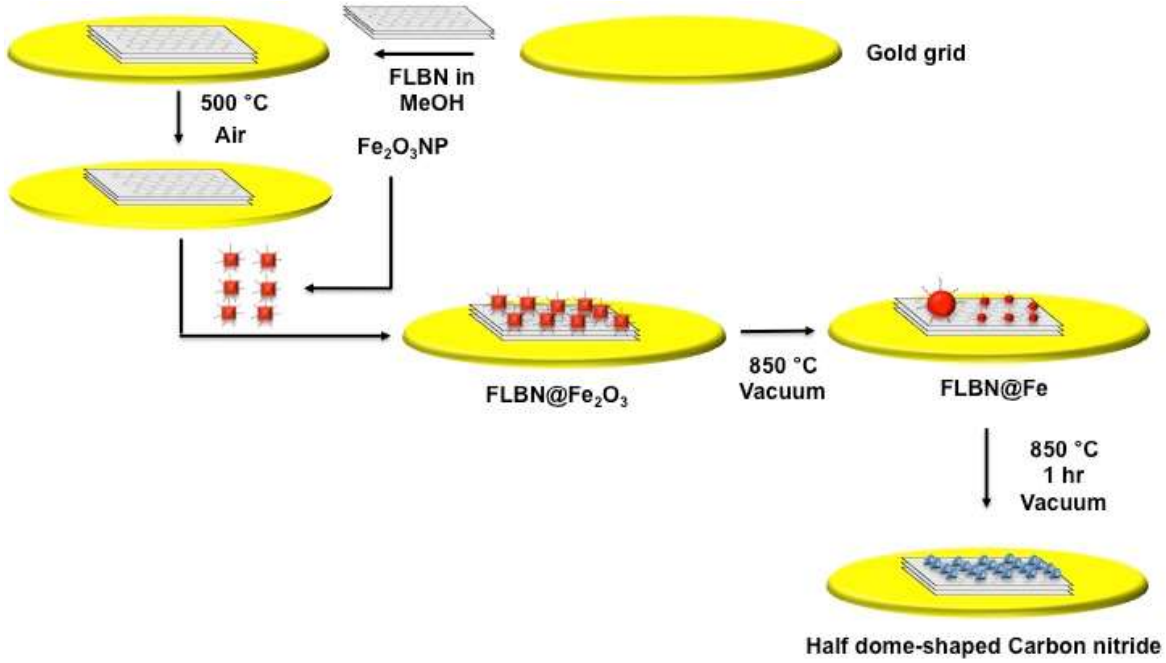

Figure 1. Schematic representation of the half dome shaped formation. (a) Few layer boron nitride sheets (FLBN) were deposited from solution on gold TEM grid. The FLBN were heated in air to remove advantageous carbon. Iron oxide nanoparticles (Fe_2O_3) synthesised in the presence of $N(CH_3)_4OH$ were deposited on freshly FLBN to form FLBN@Fe_2O_3 hybrid structure. The hybrid was heated at 850 °C in vacuum, firstly the Fe_2O_3NP were reduced to FeNP to form FLBN@Fe, secondly, the FeNP commenced the ripening processes in which smaller nanoparticles were migrating towards bigger nanoparticle. During this migration process the small nanoparticles come across the step edges of the FLBN to form during the combustion chemistry the CN@HDS.

The iron oxide nanoparticles Fe_2O_3 capped with tetra methyl ammonium hydroxide $N(CH_3)_4OH$ were deposited form solution onto freshly FLBN on a TEM grid. The TEM grid was inserted in a dedicated TEM heating stage holder and heated at 850 °C for 30 minutes (Figure 1). The TEM images clearly shows the CN@HDS protruding the iron nanoparticle (Figure 2). Under this condition, we have been able to image the formation of CN@HDS in real time. The FeNP post their reduction commenced the ripening processes in which smaller nanoparticles were migrating towards bigger nanoparticle (Figure S2b). During this migration process the small nanoparticles come across the step edges of the FLBN the CN@HDS were formed (Figures 3–5). The small nanoparticle escaped from the CN@HDS dome structure migrating towards the big nanoparticle leaving behind part of the organic

Preprints (www.preprints.org) | NOT PEER-REVIEWED | Posted: 25 September 2023 doi:10.20944/preprints202309.1317.v2

capping agent (Figure 5 video file 2). Analysing the sample after 1 hr, the CN@HDS structures were present at the step edges of the FLBN as EELS measurement clearly show a feature in the region at 284,5 eV and the K edge at 292 eV. (Figure 3b-4d and S6). Raman spectroscopy of the CN@HDS structures formed on FLBN showed a D-band and G-band at 1350 (D1) and 1593 cm^{-1} (G2), respectively (Figure S8). The Raman spectroscopy also shows an intense peak at 2200 cm^{-1} characteristic of CN sp^1 and a 2D band peak at 2700 cm^{-1} characteristic of CN sp^2.[23]

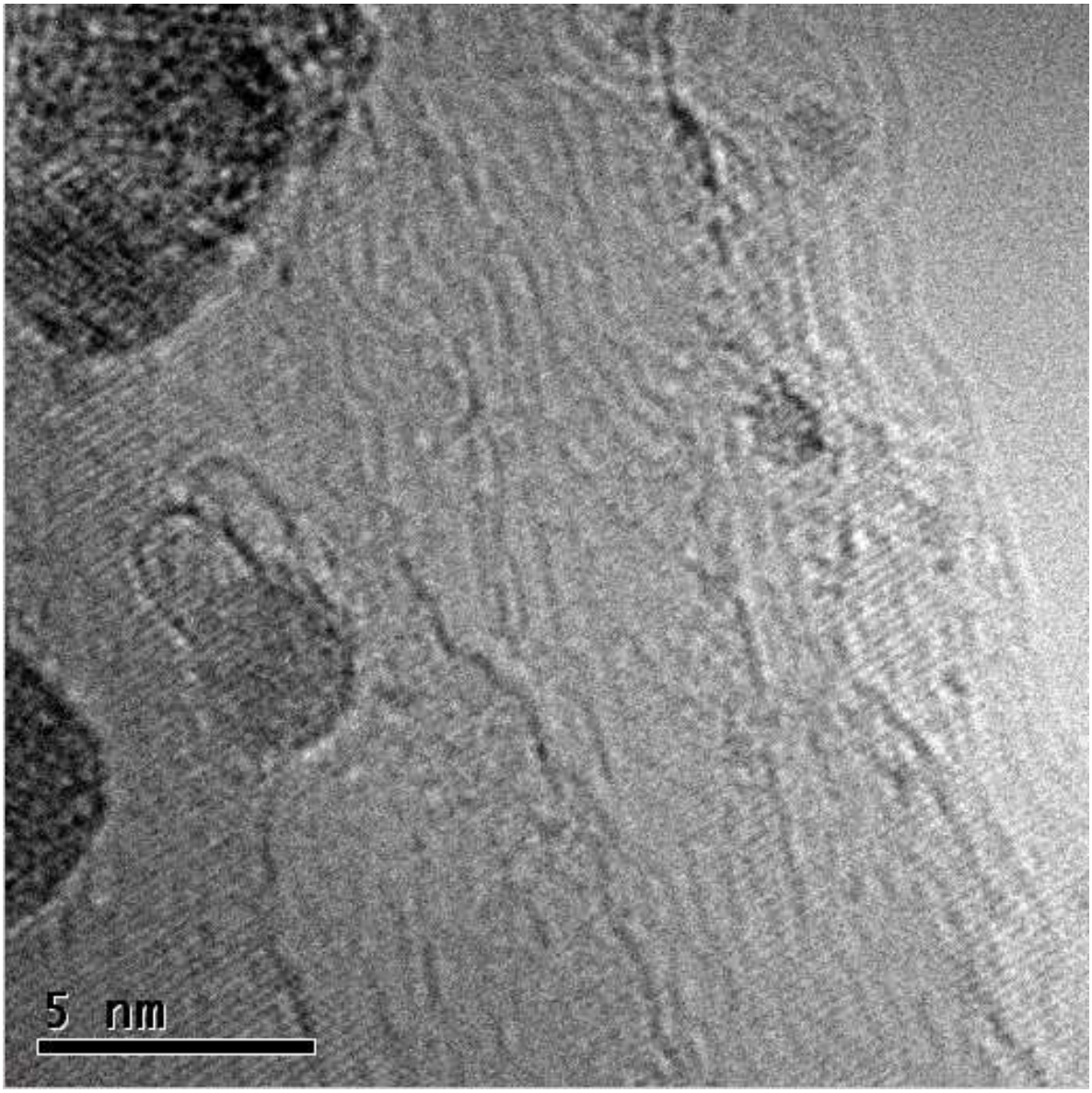

Figure 2. (a) Carbon nitride half dome structure CN@HDS protruding the iron particles (small particle, video file 1),.

Preprints (www.preprints.org) | NOT PEER-REVIEWED | Posted: 25 September 2023 doi:10.20944/preprints202309.1317.v2

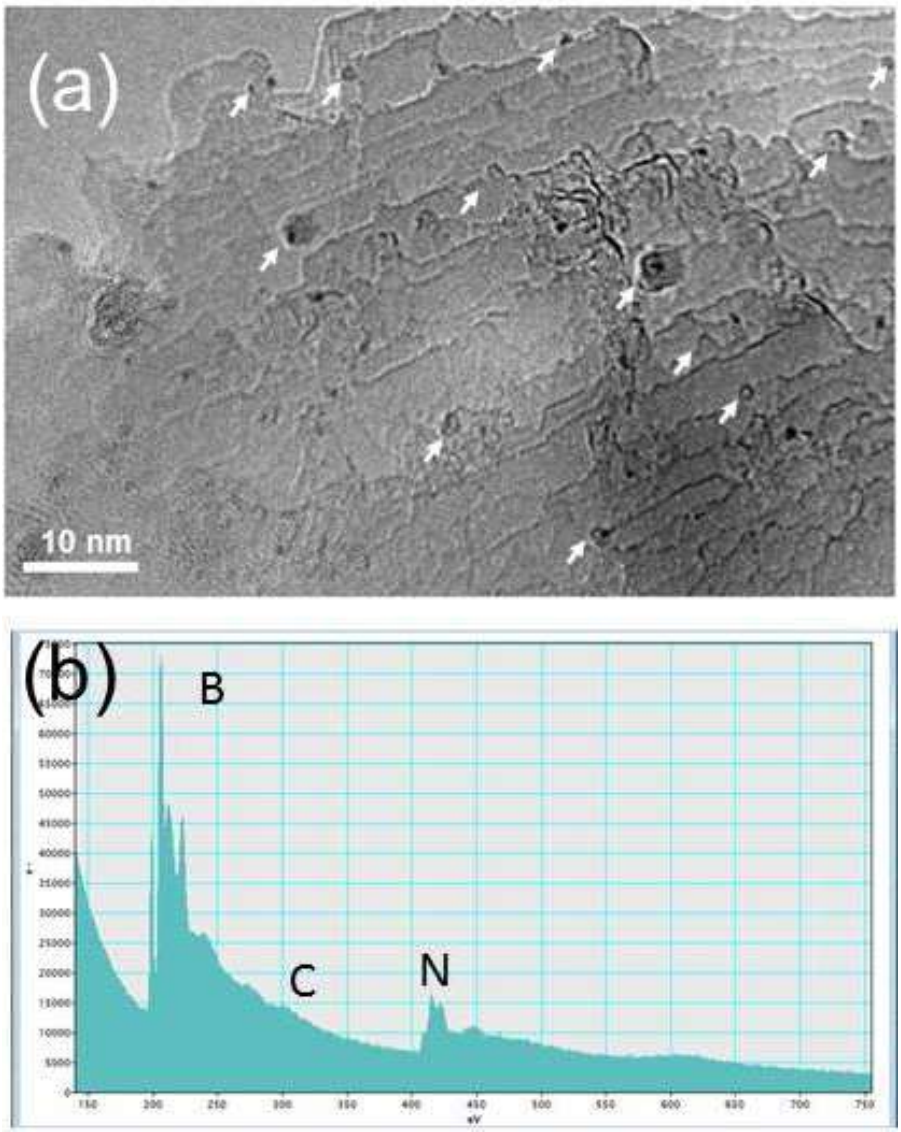

Figure 3. (a) Bright field TEM image showing the CN@HDS residing on the step edges on FLBN – image acquired at 850 °C, at c.a. 30 minutes of in situ heating in vacuum; (b) corresponding EELS of the half dome structure clearly shows the presence of the carbon peak at 284,5 eV which is weak compared to a pure carbon material, and the K-edge at 292 eV. Arrows denote CN@HDS, some of which are decorated with few atoms Fe cluster. The escape of the metal catalyst from CN@HDS is shown in real time on figure 4 and video file 2.

Preprints (www.preprints.org) | NOT PEER-REVIEWED | Posted: 25 September 2023 doi:10.20944/preprints202309.1317.v2

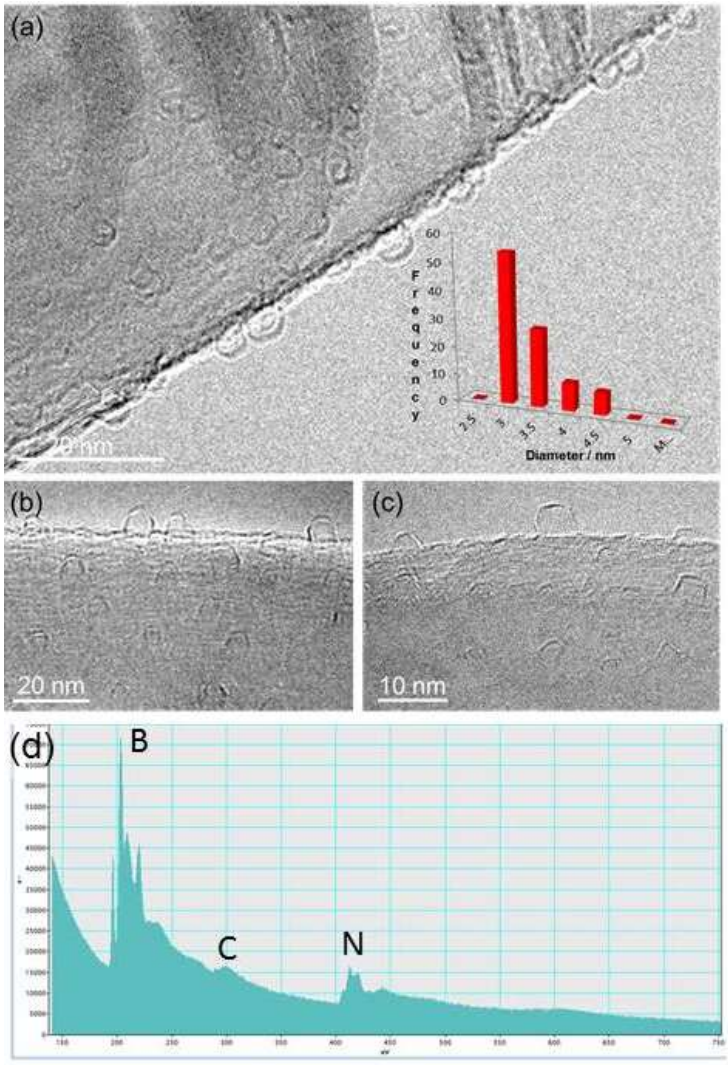

Figure 4. (a-b) TEM images show CN@HDS residing on FLBN sheets (feature size histogram as inset: diameter 2.6 - 4.4 nm). The images were taken after 1 hr heating treatment (c) TEM images of the BN@HDS half-dome structures. (a-b) EELS of the half dome structure clearly shows the presence of the carbon peak at 284,5 eV, and the K-edge is at 292 eV.

Preprints (www.preprints.org) | NOT PEER-REVIEWED | Posted: 25 September 2023 doi:10.20944/preprints202309.1317.v2

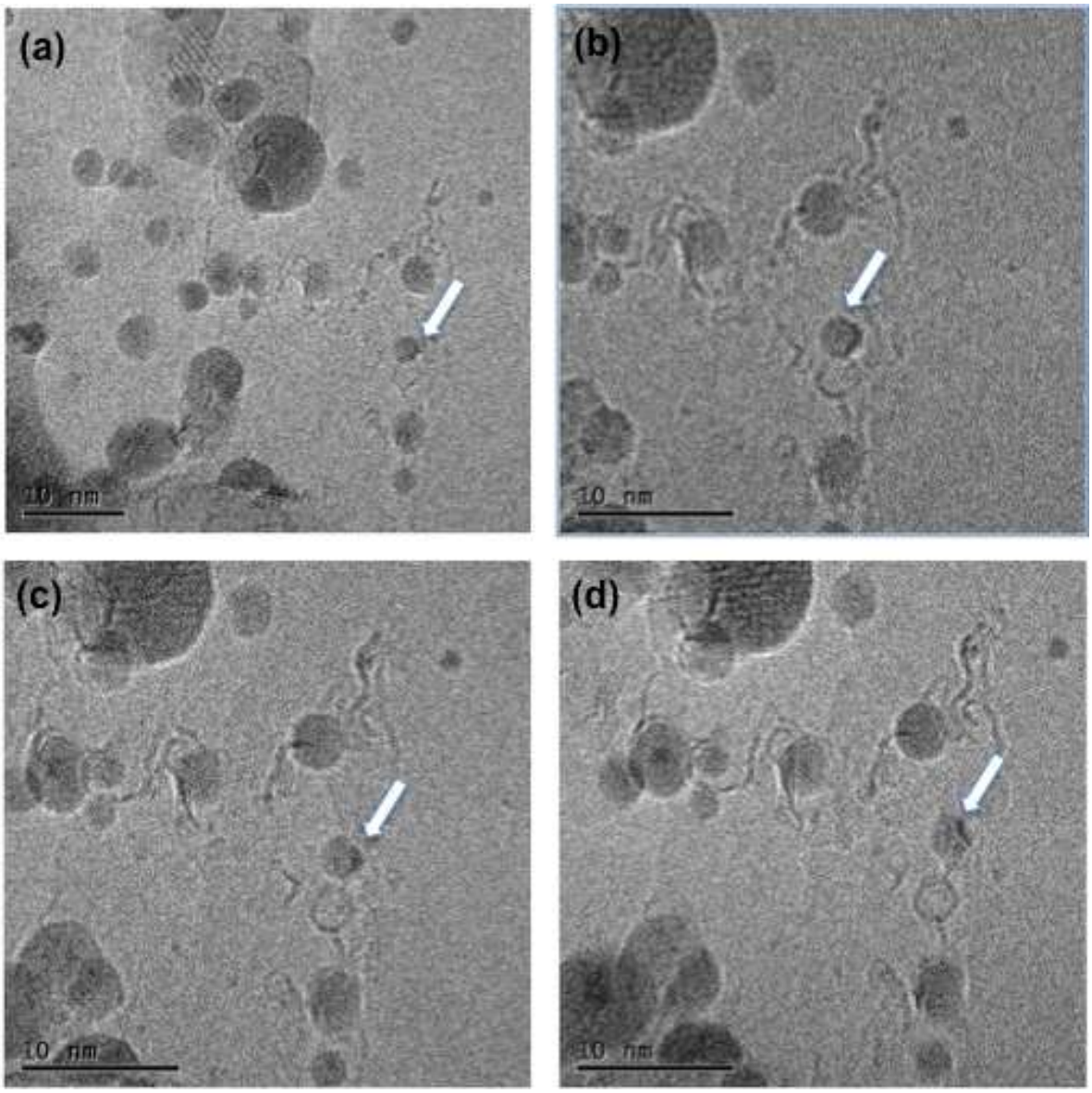

Figure 5. (a-d) Formation mechanism of CN@HDS on the step edges of few layer boron nitride sheets, it can also be seen the escape of FeNP from the CN@HDS.

In a control experiment, it was verified the possibility to form CN@HDS structure containing nitrogen using a carbon support. We have used the same heating condition for the Fe_2O_3@FLBN hybrid inside the column of a TEM microscope. Detailed STEM-EELS analysis carried out on the CN@HDS revealed the presence of nitrogen with a ratio of 1 Nitrogen atom to 4 Carbon atoms as the source of Nitrogen of the BN was not present in this experiment (Figure S4). Conversely, when the half dome structure were grown on few layer boron nitride sheets, the organic base during the combustion process catalysed by iron, reacted with the few layer boron nitride sheet allowing the uptake of nitrogen atoms to form cyanopolyynes with a ratio of 1 atom of nitrogen to 1 atom of carbon (Figure 2-5 and S9).

It was also noticed that when the nanoparticles runs out of the capping agent, they become naked and commenced to interact with the surfaces of FLBN either on the step edges or the flat surfaces to form BN@HDS. It was considered that Fe atom clusters originating from the large Fe NP's (>30 nm) diffuse and become trapped along the dangling bonds and defect sites of BN step-edges. TEM images and simulated TEM images show that the morphologies of these BN@HDS nanostructures are distinct from their carbon analogues, requiring squares, pentagons, hexagons, heptagons and octagonal rings in their formation.[48] On the contrary to the CN@HDS half dome structure, the BN-half dome structures display sharp corners and edges (Figure 4c and S12).[48]

 doi:10.20944/preprints202309.1317.v2

Discussion

Nobel metal nanoparticles has already shown the ability of catalysing the formation of carbon forms contain sp^1/sp^2 carbon as was recently shown by Kutrovskaya S. *et al.* under an effect of laser irradiation and electromagnetic fields using gold nanoparticles.[33] A similar methodology was reported by Casari *et al.*, noble metals particles have shown a high affinity to form carbon structure containing H-terminated polyyne.[34] Okada *et. al.* have shown the possibility to produce a polymeric composite containing polyyne stabilised by silver nanoparticles.[35] Carbon films enriched with carbyne species can be produced either via Chemical vapour deposition or Physical vapour deposition.[15] It has also been shown that the dechlorination of Polyvinylidene chloride formed polyyne-polyene carbon films. Recently, a new generation of N-doped carbons have been found to be interesting materials because of their superior physical and chemical properties as compared to those of their undoped counterparts. Accordingly, wide ranges of applications are anticipated for these nitrogen-doped carbon materials such as anodes in high performance lithium ion batteries, high performance supercapacitors, as an adsorbent to be exploited for removing toxic pollutants from water. In addition, carbon nitride materials can provide large number of anchoring point sites adsorption for positive charged metal ions due to the electronegativity difference between N and C atoms in CN@HDS sp^2 hybridization.[12,15,23]

The current literature report on the propensity of Nobel metals to form carbon forms containing sp^1/sp^2, the possibility that FeNPs are able to catalyse the formation of such carbon nitride forms has never been reported previously. During the temperature increase in our experiments, from 20 ˚C to 850 ˚C in vacuum, $N(CH_3)_4OH$ is expected to undergo significant structural transformations, the $N(CH_3)_4OH$ transforms to nitrile $N(CH)_3$ and CH_3OH (E2 Reaction), the alcohol evaporate and the nitriles begin its transformation forming cyano groups that reacts specifically with unsaturated carbon atoms, the support FLBN provide for a source of nitrogen atom that is required to form cyanopolyynes with the ratio of 1 carbon atom to 1 nitrogen atom (Figure S13). The unsaturated carbon formation can be explained, as C-H bonds at around 300 ˚C, begin to dissociate, transforming the alkyl chains to alkene, polyene and polyyne and cumulenic chains, thus gradually converting sp^3-hybridised carbon to sp^1-hybridised carbon. However, as sp^1 chains are predicted to react with each other,[21] the close proximity of the molecules within half dome structures in our experiments, are likely to trigger cross-linking of the chains, leading to the formation of 2D material with CN sp^2 regions interconnected by sp^1-hybridised CN chains (Figure S9) stabilised by positive charge over the nitrogen atoms. Such cross-linking immobilises the carbon material around the metal core, preventing desorption of the molecules, whilst de-hydrogenation continues as the temperature rises to 850 ˚C, thus forming CN@HDS around the FeNP.

High-resolution TEM imaging indicates that the CN@HDS are different qualitatively to other known forms of carbon nanoparticles, such as fullerenes, carbon onions, carbon black or nano-horns, showing clearly the overall hemispherical morphology of the half dome structures. We have observed that with small iron nanoparticles the CN@HDS present a single layer, conversely, when the iron particles up to 20 nm diameter the half dome multilayers structures could be observed surrounding the metal core (Figure 1b and S14). It was interesting to see that during the particle migration and coalescence of the FeNPs the capping agent still remained attached to the NPs as the solely available source of carbon in our systems is the organic base, as we have grown those CN@HDS on FLBN (BN was heated in air to removed advantageous carbon). The small Fe clusters during their migration were momentarily trapped at the step edges of the FLBN which acts as anchoring point, reaction site, and source of nitrogen atom which were uptake during the combustion that allowed the formation of the half dome structure 1 : 1 ratio (Figure 5, Video file 2). Conversely, for the big nanoparticles in which the particle migration was not shown post intense heating the carbon nitride was surrounding the nanoparticle (Figure S14).

The EELS of the half dome structures shows a weak peak at 284,5 eV which lies in the region of carbon chains and its low intensity is due to the presence of sp^1 CN.[15,23,36-37] In addition, the K-edge at 292 eV lies in the region of graphitic carbon, differing from diamond at 290 eV and amorphous carbon at 295 eV (Figure 3b-4d and S6). [36-37] The weakness of the σ* peak is due to the presence of nitrogen.[36]

 doi:10.20944/preprints202309.1317.v2

The broadness of the carbon K-edge above 292 eV (Figure 3b, 4b and S6) is unusual for pure sp^2-hybridised carbon and is comparable to that observed for materials containing sp^1 and or sp^2 carbon and carbon nitride.[36-37] The high energy EELS measurements suggest that the bonding state within the carbon matrices does not match with well-known forms of carbon, but can be explained by the presence of sp^1-hybridised CN intermixed within sp^2-CN material.[15,31,32,35-38]

In addition, the Raman of half dome (Figure S8) data shows a peak at 2200 cm^{-1} characteristic of CN sp^1 (Figure S8).[23,39] Generally, Raman spectra of carbon nitride material show a characteristic peak between 2100 and 2200 cm^{-1}.[9,15,20,23,39] The vibration frequencies of solid carbon nitrides are expected to lie close to the modes of the analogous unsaturated CN molecules, which are 1500–1600 cm^{-1} for chain like molecules and 1300–1600 cm^{-1} for ring like molecules. [40-41] This means that there is little distinction in the G-D region between modes due to C or N atoms. For example, the frequency of bond stretching skeletal and ring modes is very similar in benzene, pyridine, and pyrrole, so it is difficult to assess the presence of N in an aromatic ring. The modes in amorphous carbon nitrides are also delocalized over both carbon and nitrogen sites because of nitrogen's tendency to promote more clustered sp^2 bonding. It is expected little difference between the Raman spectra of nitrogenised and N-free carbon films in the 1000-2000 cm^{-1} region. It was found no shift in the Raman spectra of two sputtered CN samples, one with 26 % at ^{14}N and the other with the same content of ^{15}N. On the other hand, we clearly have detected a direct contribution of CN sp^1 bonds in the 2100-2200 cm^{-1} regions.[15,23,39]

In a previous study, silver nanoparticles containing $C_{12}H_{25}S$ were heated in a dedicated heating stage and post their intense heating it was shown that the sulfur contained in the organic capping agent was retained in the discorded carbon structure formed.[42] We have also heated the Fe_2O_3 capped with $N(CH_3)_4OH$ in a dedicated heating stage, post intense heating, we have also shown for the first time that nitrogen of the $N(CH_3)_4OH$ originally forming the capping agent can be retained in our CN@HDS (Figure S4 and S9).

The EELS and Raman measurements shows the presence of Nitrogen from the sp^1 CN formed during the heating process of the capping agent, the $N(CH_3)_4OH$ due to intense heating transforms to nitrile $N(CH)_3$ and CH_3OH (E2 Reaction), the alcohol evaporate and the nitrile begin its transformation forming cyano groups that reacts with unsaturated carbon atoms to form cyanopolyynes chains. The cyano radicals can react with a variety of molecules in combustion chemistry, amongst which are simple unsaturated hydrocarbons.[43-46]

The synthesis of monocyanopolyyens and dicyanopolyynes could be easily produced either by laser ablation or with arch discharge techniques.[15,47-48] For instance; two graphite electrodes were connected at the pole of the d.c. power supply and submerged in a Pyrex three-necked round bottom flask filled with acetonitrile to yield cyanopolyyens.[15] In recent years, a renewed interest in the reaction of CN radicals with simple unsaturated hydrocarbons has risen because of their alleged role in some extra-terrestrial environments, namely the atmosphere of Saturn's moon Titan and in cold molecular clouds in the interstellar medium (ISM).[15] In addition cyanopolyyne have been extensively identified in cold molecular clouds and outflow of late M-type AGB carbon stars and their production routes have been widely investigated. The interstellar medium products can be arranged in four groups cyanopolyynes, methyl substituted cyanopolyynes, cyanopolyynes radicals and olefin nitriles containing a double carbon bond and a CN group.[15]

In a previous study, A. La Torre *et al* has reported on the growth and formation of single boron nitride half dome structure BN@HDS mediated by small naked metal particle that reacted with the dangling bonds of the FLBN to form BN protrusion which display sharp corner and edges, the shape of the iron nanoparticle rearranged to a rectangular shape to promote the formation of BN@HDS (Figure 4c, S13). The formation mechanism was already presented; two mechanisms can be accepted. One possibility is the dissolution-precipitation mechanism, whereby BN dissociates on the surface of the Fe clusters (noting B and N atoms are soluble in Fe)[29–31], followed by dissolution, diffusion and precipitation of BN in a form of dome-shaped nanostructures in advance of loss of the Fe at elevated temperature. This is similar to the case of carbon nanostructures, where the nucleation of protrusions on the surfaces of metal atom clusters can occur.[29] The second possibility is the "scooter" mechanism,

 doi:10.20944/preprints202309.1317.v2

as proposed to explain the growth of carbon nanotubes.[29] Here, mobile Fe atoms could continue to etch the BN layers in such a way that small strips remain that subsequently curl and close to form dome-shaped nanostructures. After nanostructure closure, the Fe atoms may either remain trapped inside the cage or escape, depending on the heating conditions or on the experimental conditions.[29]

This new CN@HDS discovered in our study, might combines the features of graphene and carbyne as they can also be grown on graphene, and offers significant potential for a wide variety of applications. These CN@HDS are found to be very stable under ambient conditions in air or at high temperature in vacuum, exhibiting no measurable structural deterioration in our experiments, and thus being as robust as graphene and or diamond. Recently, we have reported on a new form of nanoscale carbon in the shape of hemispherical matrices with the bonding characteristics of either sp^1 or sp^2 carbon.[49] The carbon matrices were formed spontaneously at high temperature from organic molecules adsorbed on the surface of silver nanoparticles, with the metal core acting simultaneously as catalyst and template for the carbon matrices growth. Significantly, this new form of carbon exhibits photo luminescent activity in the visible and near-IR ranges, with the wavelength of emitted light determined by the length of sp^1 chains which link sp^2 domains.[49] The optical and electron properties of carbon chains and Nano ribbons are well known, the optical properties of sp^2 carbon nitride has already been reported in literature showing an upper limit at c.a. 680 nm,[23] hence, we speculate that the half dome structure could potentially present interesting photoluminescence properties ranging from the NIR range to the UV depending on the cyanopolyyne chain length.[23,49]

Last but not least, we should be taking into consideration the formation of a ternary domain by exploring the heating rate condition of Fe_2O_3@FLBN hybrid structure as the Iron particle is able to solubilise carbon, boron and nitrogen, hence it would also be possible to form pentagonal BCN monolayers or even BN chains as it was also reported by Cretu *et al.*,[21] perhaps linear chains of BCN would be a possibility in the near future.

Experimental Methods

The TEM data sets were acquired using a JEOL 2100F (point resolution 0.19 nm; accelerating voltage 200 kV) with aberration-corrected probe and Gatan imaging filter (GIF) for electron energy loss spectroscopy (EELS) at the Institut de Physique et Chimie des Matériaux de Strasbourg, France; and a JEOL 2100F (point resolution 0.19 nm; accelerating voltage 200 kV) equipped with a Gatan Tridiem imaging filter for EELS at the Nanoscale and Microscale Research Centre, University of Nottingham, U.K. A Gatan 652 double-tilt heating holder was used for the in situ TEM heating experiments. The SEM data sets were acquired using an FEI Quanta 200 3D at an accelerating voltage of 5-10 kV and working distance of 15 mm, using secondary imaging mode, at the Nanoscale and Microscale Research Centre in Nottingham; and a Jeol 6700F at the Institut de Physique et Chimie des Matériaux de Strasbourg.

Nanoparticles of iron oxide were produced using the following standard procedure. 10 mL of 1 M $FeCl_3$ solution was mixed with 2.5 mL of 2 M $FeCl_2$ solution in a flask. The mixture was heated to 70°C under Ar, with mechanical stirring, and then 21 mL of 25% $N(CH_3)_4OH$ aqueous solution was drop wise cast into the mixture. The resulting Fe_2O_3 nanoparticles (Figure S4), with associated particle size histogram measured by SEM were isolated using a permanent magnet, allowing the supernatant to be decanted. Degassed water was then added to wash the precipitates. This procedure was repeated four times to remove excess ions and the tetramethylammonium salt from the suspension. The remaining precipitate was freezing dried to create a powder.

TEM supports were prepared by drop-casting a commercially available methanolic suspension of FLBN (Graphene Supermarket; lateral size of 50-200 nm and thickness of 1-5 monolayers) onto a gold mesh TEM grid and heating in air at 550°C in a tube furnace to remove adventitious carbon. The Fe_2O_3 NP were suspended in methanol and dropped on to the BN flake / gold mesh grids. The Fe_2O_3/FLBN were heated in a dedicated heating stage holder in a TEM in situ.

TEM grids were prepared by drop casting a commercially available methanolic suspension of few layers graphene (Graphene supermarket). The Fe_2O_3NP were suspended in methanol and

dropped on to the FLG flake / gold mesh grids. The TEM support containing FLG and Fe_2O_3 were heated in a dedicated heating stage holder in a TEM in situ.

Raman spectra were recorded using a Horiba–Jobin–YvonLabRAM Raman microscope, with a laser wavelength of 633 nm operating at low power (*ca.* 4 mW) and a 600-lines/mm grating. The detector was a Synapse CCD detector. Spectra were collected by recording 64 acquisitions of 5 s duration for each spectral window. Three spectra were recorded for each sample in order to account for sample in homogeneity. The Raman shift was calibrated using the Raleigh peak and the 520.7 cm^{-1} silicon line from a Si (100) reference sample.

Acknowledgements: The author would like to thank Drs M. W. Fay and F. Ben Romdhane for carrying EELS experiments, Dr. G. A. Rance for carrying the Raman measurements, J. Jouhannaud for the synthesis of the Fe_2O_3.The author would like to thank Professors Paul Brown, Andrei Khlobystov, Genevieve Pourrey, Elena Besley, and Florian Banhart for discussion. The author acknowledges the support of the TEM and complementary techniques at the NMRC at Nottingham and at the Institut de Physique et Chimie des Matèriaux de Strasbourg, UMR 7504 CNRS, Université de Strasbourg, 23 rue du Loess, 67034 Strasbourg, France.

Abbreviations:

FLBN Few layer boron nitride
FLG few layers graphene
NP nanoparticles
FeNP Iron nanoparticles
Fe_2O_3NP Iron oxide nanoparticles
h-BN Hexagonal boron nitride
EELS Electron energy loss spectroscopy
STEM scanning transmission electron microscopy
TEM Transmission electron microscopy
CN carbon nitrides
HDS half dome structures
HDS@CN half dome structures carbon nitrides
HDS@BN half dome structures boron nitride
PTFE polytetrafluoroethylene
TEM transmission electron microscope
HRTEM high-resolution transmission electron microscope
CCD charge-coupled device
ISM Interstellar medium
GIF Gatan imaging filter

References

1. Terrones, H.; Terrones, M.; Hernandez, E.; Grobert, N.; Charlier, J. C.; Ajayan, P. M.; New metallic allotropes of planar carbon. *Phys. Rev. Lett.*, ***84***, 1716-1719, (2000).
2. Endo, M.; Muramatsu, H.; Hayashi, T.; Kim, Y. A.; Terrones, M.; Dresselhaus, M. S.; 'Buckypaper' from coaxial nanotubes, *Nature*, ***433***, 476, (2005).
3. Iijima, S.; Ichihashi, T.; Single-shell carbon nanotubes of 1-nm diameter, *Nature*, ***363***, 603-605, (1993),
4. Chuvilin, A.; Kaiser, U.; Bichoutskaia, E.; Besley, N. A.; Khlobystov, A. N.; Direct transformation of graphene to fullerene, *Nature Chemistry*, ***2***, 450-453, (2010).
5. Goroff, N. S.; Mechanism of Fullerene Formation, *Acc. Chem. Res.*, ***29***, 77-83, (1996).
6. Kroto, H. W.; McKay, K.; The formation of quasi-icosahedral spiral shell carbon particles, *Nature*, ***331***, 328-331, (1988).
7. Sharma, R.; Rez P.; Treacy, M. M. J.; Stuart, S. J.; In situ observation of the growth mechanism of carbon nanotubes under diverse reaction conditions. *J. Electron Microsc.*, ***54***, 231-237, (2005).
8. Eckmann, A.; Felten A.; Mishchenko, A.; Britnell, L.; Krupke, R.; Novoselov, K. S.; Casiraghi, C.; *Probing the nature of defects in graphene by Raman spectroscopy. Nano Lett.*, ***12***, 8, 3925-3930, (2012).
9. Charlier, J-C.; Defects in Carbon Nanotubes. *Acc. Chem. Res.*, ***35***, 12, 1063-1069, (2002).
10. Malko, D.; Neiss, C.; Vines, F.; Görling, A.; Competition for graphene: graphynes with direction-dependent dirac cones. *Phys Rev Lett.*, ***108***, 086804, (2012).

11. Peng, Q.; Dearden, A.; Crean, J.; Han, L.; Liu, S.; Wen, X.; De, S.; Nanotechnology, New materials graphyne, graphdiyne, graphone, and graphane: review of properties, synthesis, and application in nanotechnology. *Science and Applications*, ***7***, 1-29, (2014).
12. Osswald, S.; Yushin, G.; Mochalin, V.; Kucheyev, S.O.; Gogotsi, Y.; Control of sp^2/sp^3 Carbon Ratio and Surface Chemistry of Nanodiamond Powders by Selective Oxidation in Air., *J. Am. Chem. Soc.*, ***128***, 35, 11635-11642, (2006).
13. Kroto, H. W.; Health, J. R.; O'Brien, S. C.; Curl, R. F.; Smalley, R. E. "C_{60}: Buckminsterfullerene", *Nature*, **318**, *162-163*, (1985).
14. Artyukhov, V. I.; Liu, M.; Yakobson, B. I.; Mechanically induced metal insulator transition in carbyne, *Nano Lett.*, ***14***, 4224-4229, (2014).
15. Cataldo, F.; Polyyenes: Synthesis, Properties and Characterization, CRC press, Taylor and Francis, (2006).
16. Heimann, R. B.; Evsyukov, S. E.; Kavan, L.; Carbyne and Carbynoid Structures (Kluwer Academic Publishers), (1999).
17. Baughman, R.; Dangerously seeking linear carbon, *Science*, ***312***, 1009-1010, (2006).
18. La Torre, A.; Botello-Mendez, A.; Baaziz, W.; Charlier, J.-C.; Banhart, F.; Strain-induced metal semiconductor transition observed in atomic carbon chains. *Nat. Comm.*, ***6***, 6636, (2015).
19. La Torre, A.; Ben Romdhane, F.; Baaziz, W.; Janowska, I.; Pham-Huu, C.; Begin-Colin, S.; Pourroy, G.; Banhart, F.; Formation and characterisation of carbon metal contacts, *Carbon*, ***77***, 906-911, (2014).
20. Banhart, F.; La Torre, A.; Ben Romdhane, F.; Cretu O.; The potentials and challenges of electron microscopy in the study of atomic chains, *The European Physical Journal Applied Physics*, ***78***, 20701, (2017).
21. Cretu, O.; Komsa, H-P.; Lehtinen, O.; Algara-Sillen, G.; Kaiser, U.; Suenaga, K.; Krasheninnikov, A.; *Experimental Observation of Boron Nitride Chains*, *ACS Nano*, ***8***, 12, 11950-11957, (2014).
22. Tarakeshwar, P.; Buseck, P. R.; Kroto, H. W.; Pseudo carbynes: charge-stabilised carbon chains, *Journal of Physical Letters*, ***7***, 1675, (2016).
23. Kundu, S.; Chowdhury, I. H.; Naskar, M. K.; Nitrogen-Doped Nanoporous Carbon Nanspheroids for selective Dye Adsorption and Pb(II) Ion Removal from waste water, *ACS Omega*, ***3***, 9888-9898, (2018).
24. Chechin, G. M.; Sizintsev, D. A.; Usoltsev, O. A.; *Computational materials science*, ***138***, 353-367, (2017).
25. Benguediab, S.; Tounsi, A.; Zidour, M.; Semmah, A.; *Chirality and scale effects on mechanical buckling properties of zig-zag double walled carbon nanotubes*, *Composites Part B, Engineering*, ***57***, 21-24, (2014).
26. *Gonze, X.; Amadon, B.; Anglade, P.-M.; Beuken, P.; Bottin, F.; Boulanger, P.; Bruneval, F.; Caliste, D.; Caracas, R.; Coté, M., Deutsch, T.; et al Computer Physics Communication*, ***180***, 12, 2582-2615, (2020).
27. Chechin, G. M.; Sakhnenko, V. P.; Interactions between normal modes in nonlinear dynamical systems with discrete symmetry. *Exact results, Physica D., Non linear Phenomena*, **117**, 1-4, 43-76, (1998).
28. Chechin, G. M.; Gnezdilov, A. V.; Zekhster, M. Yu; *Existence and stability of bushes of vibrational modes for octahedral mechanical systems with Lennard-Jones potential. Int. J. Nonlinear Mech.*, 1451-1472, (2003).
29. La Torre, A.; Åhlgren, E.H.; Fay, M. W.; Ben Romdhane, F.; Skowron, S. T.; Parmenter, C.; Davies, A. J.; Jouhannaud, J.; Pourroy, G.; Khlobystov, A. N.; Brown, P. D.; Besley, E.; Banhart, F.; Growth of single layer boron nitride dome-shaped nanostructures catalysed by iron clusters, *Nanoscale*, **8**, 32, 15079-15085, (2016).
30. Kireev, D.; Liu, S.; Jin, H.; Xiao, T. P.; Bennett, C. H.; Akinwande, D.; Incorvia, J. A. C.; Metaplastic and energy-efficient biocompatible graphene artificial synaptic transistors for enhanced accuracy neuromorphic computing, *Nature Communications*, **13**, 4386, (2022).
31. Park, D-W; Schendel, A. A.; Mikael, S.; Brodnick, S. K.; Richner, T. J.; Ness, J. P.; Hayat, M. R.; Atry, F.; Frye, S. T.; Pashaie, R.; Thongpang, S.; Ma, Z.; Williams, J. C.; Graphene-based carbon-layered electrode array technology for neural imaging and optogenetic applications, *Nature Communications*, **5**, 5258, (2014).
32. Reich, S.; Ferrari A. C.; Arenal R.; Loiseau A.; Bello I.; Robertson J.; *Resonant scattering in cubic and hexagonal boron nitride*, *Phys. Rev. B*, ***71***, 205201, (2005).
33. Kutrovskaya, S.; Samyshkin, V.; Lelekova, A.; Povolotskiy, A.; Osipov A.; Arakelian S.; Kavokin A. V.; Kucherik A.; *Nanomaterials*, ***11***, 763, (2021).
34. Casari, C. S.; Li Bassi, A.; Baserga, A.; Ravagnan, L.; Piseri, P.; Lenardi, C.; Tommasini, M.; Milani, A.; Fazzi, D.; Bottani C. E.; Milani, P.; Low-frequency modes in the Raman spectrum of sp−sp^2 nanostructured carbon, *Physical Review B*, ***77***, 195444, (2008).
35. Okada, S.; Fuijj, M.; Hayashi, S.; Immobilization of polyynes adsorbed on Ag nanoparticles, *Carbon*, ***49***, 4704, (2011).
36. Merchant, A.R.; *et al.* Structural Investigation of two carbon nitride solids produced by cathode arc deposition and nitrogen implantation AU9716187 Electron microscopy Unit and School of Physics University of Sydney, Australia.
37. Hu, J.; Yang, P.; Lieber, C. M.; Nitrogen driven structural transformation in carbon nitride material, *Applied Surface Science*, ***127-129***, 596-573, (1998).
38. Lin, Y-C.; Morishita, S.; Koshino, M., Yeh, C-H.; Teng, P-H., Chiu, P-W., Hidetaka Sawada, H.; Suenaga, K.; Unexpected Huge Dimerization Ratio in One-Dimensional Carbon Atomic Chains, *Nanoletters*, ***17***, 494-508, (2017).

39. Ferrari, A. C.; Rodil, S. E; Robertson J.; *Physical Review*, ***B67***, 155306, (2003).
40. Dollish, F. R.; Fateley, W. G.; Bentley, F. F.; *Characteristic Raman Frequencies of Organic Molecules* Wiley, New York, (1974).
41. *Physical Methods in Heterocyclic Chemistry*, edited by Katkritzki A. R., Academic, New York, 1963 ; Vols. II, IV.
42. Watts, J. A.; Fay, M. W.; Rance, G. A.; Khlobystov, A. N.; Brown, P. D.; Carbon Formation of hollow carbon Nano shells from thiol stabilised silver nanoparticles via heat treatment, *Carbon*, ***139***, 538-544, (2018).
43. Yang, D. L.; Lin, M. C.; The reaction of the CN radicals with molecules relevant to combustion and atmospheric chemistry. In: The Chemical Dynamics and Kinetics of small radicals – *Advanced series in Physical Chemistry*, K. Liu, A. Wagner, Eds. World Scientific, Singapore, ***6***, 164-213, (1998).
44. Yang, D. L.; Lin, M. C.; The reaction of CN radical reactions with selected olefins in the temperature-range 174 K-740 K, *Chem. Phys.*, ***160***, 317-325, (1992).
45. Sims, I. R.; Queffelec, J. L.; Travers, D.; Rowe, B. R.; Herbert, L. B.; Karthauser, J.; Smith, I. W. M.; Rate constant for the reaction of CN with hydrocarbons at low and ultra-low temperatures. *Chem. Phys. Lett*, ***211***, 461-468, (1993).
46. Choi, N.; Blitz, M. A.; McKee, K.; Pilling M. J.; Seakins P. W.; H atom branching ratios from the reaction of CN radicals with C_2H_2 and C_2H_4, *Chem. Phys. Lett.*, ***384***, 68-72, (2004).
47. Grosser, T.; Hirsch, A.; Synthesis of Cyanopolyynes. *Angew. Chem. Int. Ed. Engl.*, ***32***, 1340, (1993).
48. Gibtner, Th.; Hampel, F.; Gisselbrecht, J. P.; Hirsch, A.; End-cap stabilised oligoneys: model compounds for the linear sp carbon allotrope Carbyne. *Chem. Eur. J.*, ***8***, 48, (2002).
49. A. La Torre, Research Square, doi.org/10.21203/rs.3.rs-3292971/v1